Split-Step Simulations of Sonic Boom Propagation Beyond the Lateral Cutoff in a Turbulent Atmosphere

Alexander N. Carr[1*], Joel B. Lonzaga[1], and Steven A. E. Miller[2]

1. NASA Langley Research Center
2. University of Florida

* alexander.carr@nasa.gov

2aCA2
183rd Meeting of the Acoustical Society of America
December 6, 2022

Acknowledgements

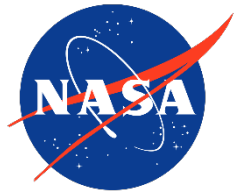

- This research was supported by the Commercial Supersonic Technology Project of the National Aeronautics and Space Administration under Grant No. 80NSSC19K1685.

- Thanks to Will Doebler, Alexandra Loubeau, Sriram Rallabhandi and others at the NASA Langley Structural Acoustics Branch for advice and guidance.

Sonic Boom Prediction Capabilities

- Several regions of sonic boom carpet due to atmospheric stratification
- Current prediction tools have difficulty beyond primary carpet
  - Geometrical acoustics not applicable [1,2]
  - Propagation sensitive to near-ground wind and temperature gradients
  - Turbulence [3-6]
- Diffraction important at cutoff
- We want to avoid parabolic approximation

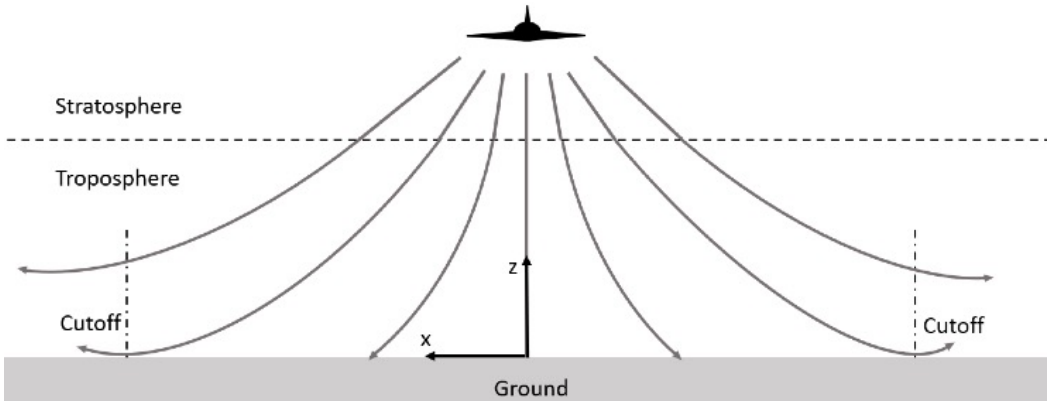

Illustration of ray path propagation from source to ground along the lateral width of the carpet.

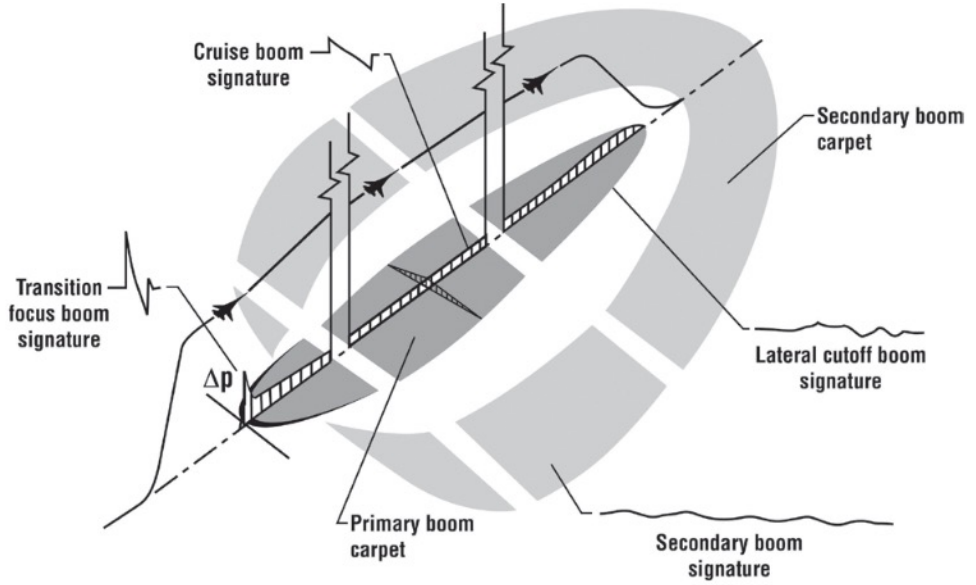

Illustration of sonic boom carpet region.

Community Noise

- Community response surveys to be conducted with X-59
  - Model dose-response relationship
  - Dose = sonic boom loudness metric (PL, ISBAP, A, B, D, E-SEL) [7]
- Previous flight tests
  - Survey techniques and measurements (WSPR [8], QSF18 [9])
  - Turbulence effects (SonicBAT [10])
  - Mach and lateral cutoff (FaINT [11,12])
- NASA FaINT
  - Typical sonic boom metrics may not be appropriate beyond cutoff
  - Lateral cutoff should be defined by acoustic threshold (suggested 65 PL_{SEL})
- Reports of booms heard beyond the cutoff in QSF18
  - How important for shaped booms, like X-59?
  - How does turbulence affect dose variability beyond cutoff?

Artist's illustration of the NASA X-59.

Objective

Problem

- Lack of understanding of shaped boom loudness (dose) levels in shadow zone
- Current prediction tools have difficulty predicting sonic boom beyond lateral cutoff

Objectives and Method

- Establish prediction method beyond cutoff with new propagation tool
- Account for turbulence effects
- Retain accuracy of lowest order diffraction term with angular spectrum approach

Outcomes

- Qualitative understanding that dose levels increase in shadow zone with increasing convection level of turbulence
- Predictions of dose uncertainty due to turbulence effects beyond lateral cutoff

Simulation Approach

- Simulation steps
  1. Propagation from source to z_i (PCBoom)
  2. Propagation from z_i to lateral cutoff (not covered here)
  3. Generate atmospheric boundary layer mean flow
  4. Simulate through 250 realizations of turbulence
  5. Extract waveforms, compute sonic boom metrics

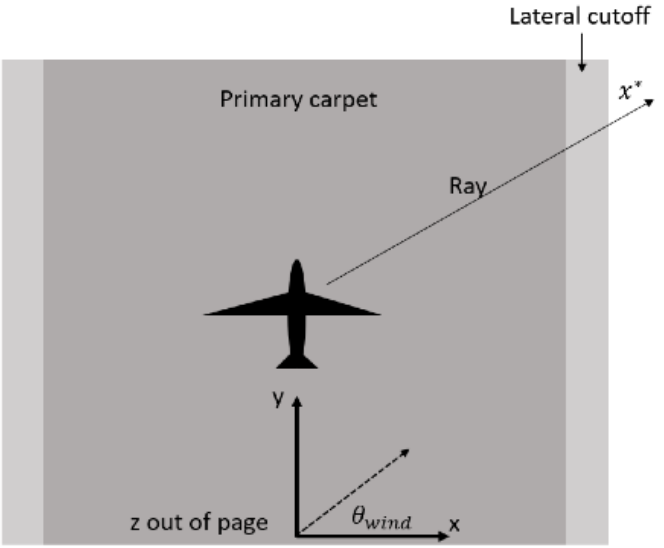

Illustration of ray path propagation to cutoff with ABL coordinates, ray coordinates, and wind direction.

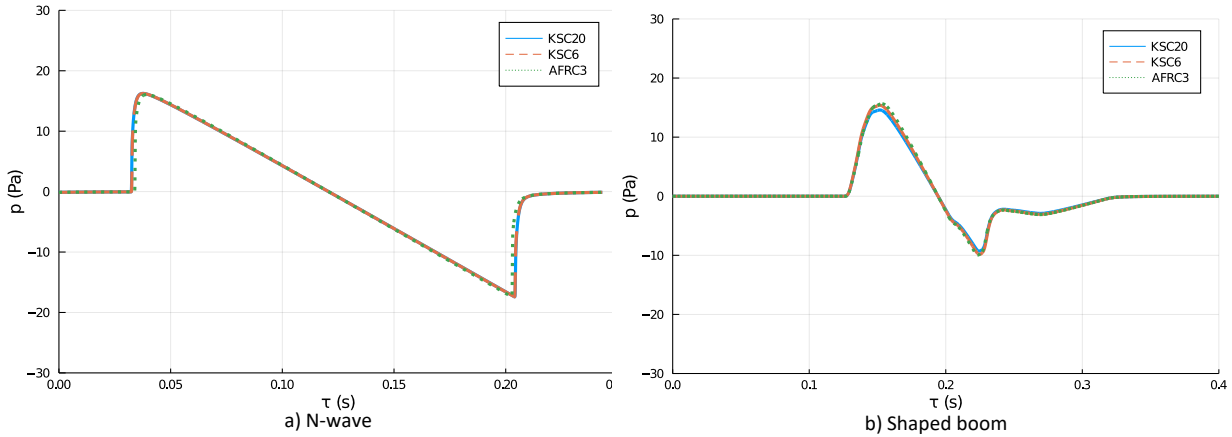

Initial waveforms at the top of the ABL used as input to propagation simulations.

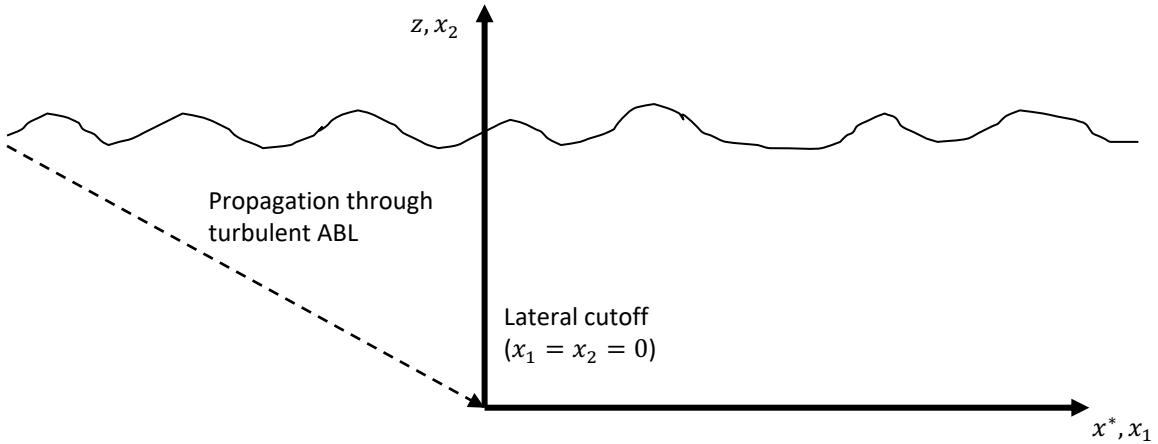

Coordinate system for lateral cutoff simulations.

Numerical Method

- Coulouvrat [13] and Ostashev [14]

$$\frac{1}{\breve{c}^2}\frac{\breve{D}^2 p}{\breve{D}t^2} - \breve{\rho}\frac{\partial}{\partial x_i}\left(\frac{1}{\breve{\rho}}\frac{\partial p}{\partial x_i}\right) = -2\frac{\partial \breve{u}_j}{\partial x_i}\int_{-\infty}^{t}\frac{\partial^2 p}{\partial x_i \partial x_j}dt' + \frac{\delta}{\breve{c}^4}\frac{\partial^3 p}{\partial t^3} + \frac{\beta}{\breve{\rho}\breve{c}^4}\frac{\partial^2 p^2}{\partial t^2} \quad (1)$$

- Partially one-way equation (Luquet [5])

$$\frac{\partial^2 p}{\partial x_1 \partial \tau} = \mathcal{D}(p) + \mathcal{H}(p) + \mathcal{N}(p) + \mathcal{A}(p) \quad (2)$$

- Integrate forward in x_1 with split-step method

$$p(x_1 + \Delta x_1, x_2, \tau) = p^{\mathcal{N}}_{\Delta x_1/2} p^{\mathcal{H}+\mathcal{A}}_{\Delta x_1/2} p^{\mathcal{D}}_{\Delta x_1} p^{\mathcal{H}+\mathcal{A}}_{\Delta x_1/2} p^{\mathcal{N}}_{\Delta x_1/2} \quad (3)$$

- Parabolic approximation only on $\mathcal{H}$

Numerical Method

- Diffraction: Angular spectrum method [15] (Accurate at all forward angles)
- Heterogeneities: Two methods
  - Exact solution of ODE involving terms with x_1 and τ derivatives
  - Crank-Nicolson integration of remaining terms
- Nonlinearities: Burgers-Hayes algorithm [16]
- Atmospheric absorption: Compute attenuation assuming no dispersion
- Validated with benchmark problems
- Agreement within 2% of analytical solutions

Daytime Atmospheric Boundary Layer

- Daytime ABL has 3 layers
  - Surface layer: strong wind and temperature gradients
  - Mixed layer: constant $\bar{u}, \bar{T}$, homogeneous turbulence
  - Inversion layer: temperature inversion, intermittency
- Will consider 3 different convection levels
  - Weak convection: $\log(-z_i L_o^{-1}) \leq 0.5$ (KSC)
  - Moderate convection: $0.5 < \log(-z_i L_o^{-1}) < 1.5$ (KSC)
  - Strong convection: $\log(-z_i L_o^{-1}) \geq 1.5$ (AFRC)

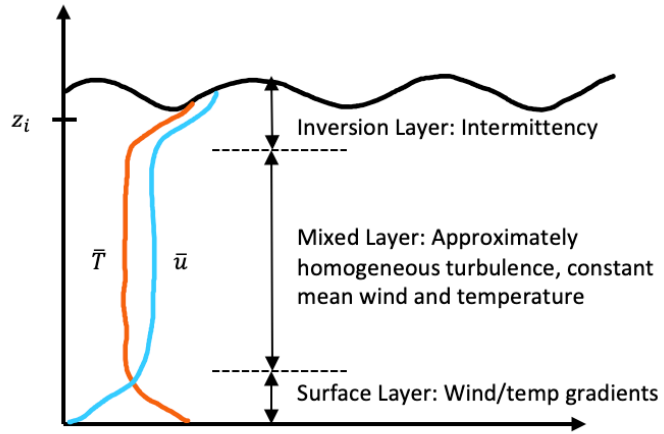

Illustration of daytime ABL.

- Obukhov length, L_o, is a measure of production of TKE due to shear and buoyancy effects

Turbulence statistics in the mixed layer.

Flight No.	σ_T (K)	L_T (m)	σ_u (m/s)	L_u (m)	z_i (m)	$\log(-z_i L_o^{-1})$
KSC20	0.044	68.30	0.67	78.30	411.6	0.115
KSC6	0.406	65.20	1.11	96.70	457.3	1.342
AFRC3	0.327	188.4	1.41	302.6	1344.0	2.459

Surface Layer Gradients

- Model surface layer gradients with MOST [17]
- Effective sound speed: $\bar{c}_{eff}(z) = \bar{c}(z) + \bar{u}(z)\cos(\theta)$
- Inhomogeneous: statistics vary with altitude
- Turbulence model (Ostashev and Wilson [18])
  - Temperature fluctuations

$$\frac{\sigma_T^2(z)}{T_*^2} = \frac{4}{(1-10\zeta)^{2/3}} \qquad \frac{L_T(z)}{z} = 2\frac{1-7\zeta}{1-10\zeta} \tag{4}$$

  - Shear driven

$$\frac{\sigma_s^2}{u_*^2} = 3.0 \qquad \frac{L_s}{z} = 1.8 \tag{5}$$

  - Bouyancy driven

$$\frac{\sigma_b^2}{w_*^2} = 0.35 \qquad \frac{L_b}{z_i} = 0.23 \tag{6}$$

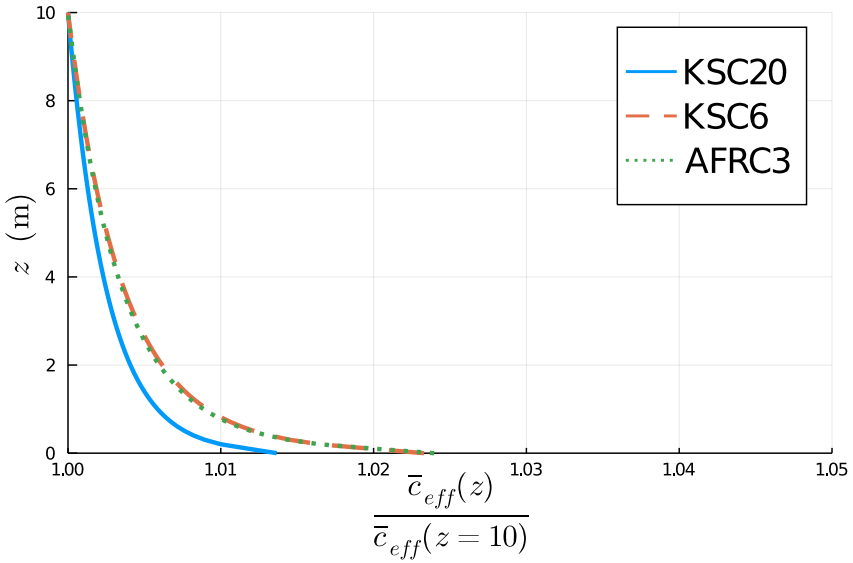

Profiles of effective sound speed near the ground for each ABL setpoint.

Generalized Random Phase Method

- Consider POD [19]

$$\int \hat{R}_{ij}(k_x, z, z')\phi_j^{(m)}(k_x, z')dz' = \lambda^{(n)}(k_x)\phi_i^{(n)}(k_x, z) \quad (7)$$

- Use eigenvalues to construct turbulent field

$$\hat{u}_i'(k_x, z) = \sum_{n=1}^{N} \lambda^{(n)}(k_x)\phi_i^{(n)}(k_x, z) \quad (8)$$

- Inverse Fourier transform to obtain $u_i'(x, z)$
- von Kármán model for $\hat{R}_{ij}(k_x, z, z')$ [20,21]
- $\sigma_u^2 = \sigma_b^2 + \sigma_s^2$
- $L_u = \left(\sigma_b^2 L_b + \sigma_s^2 L_s\right)/\sigma_u^2$

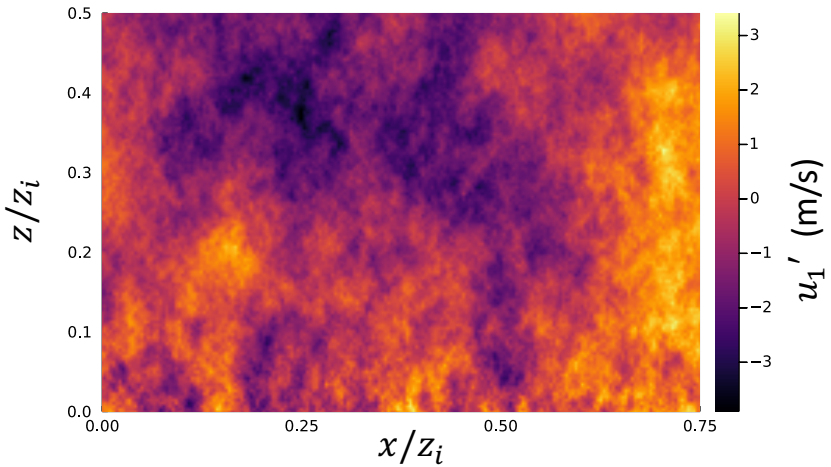

Turbulent velocity field generated in strong convection conditions.

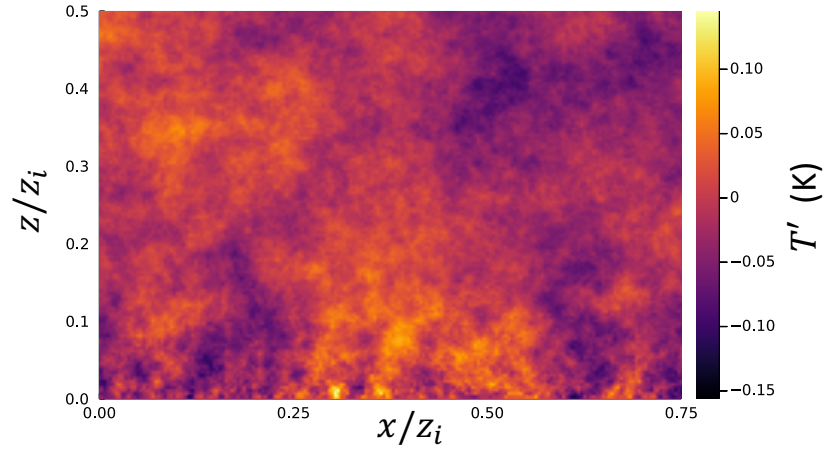

Turbulent temperature field generated in strong convection conditions.

Shadow Zone in ABL Turbulence

- Single realizations of N-wave overpressure
- Significant amplitude attenuation along x_1
- As convection level increases
  - Increased turbulent scattering
  - Increased $\overline{\Delta \mathrm{PL}}$
- $\Delta \mathrm{PL} = \mathrm{PL}(\mathrm{x}_1) - \mathrm{PL}(\mathrm{x}_1 = 0)$

Weak Convection

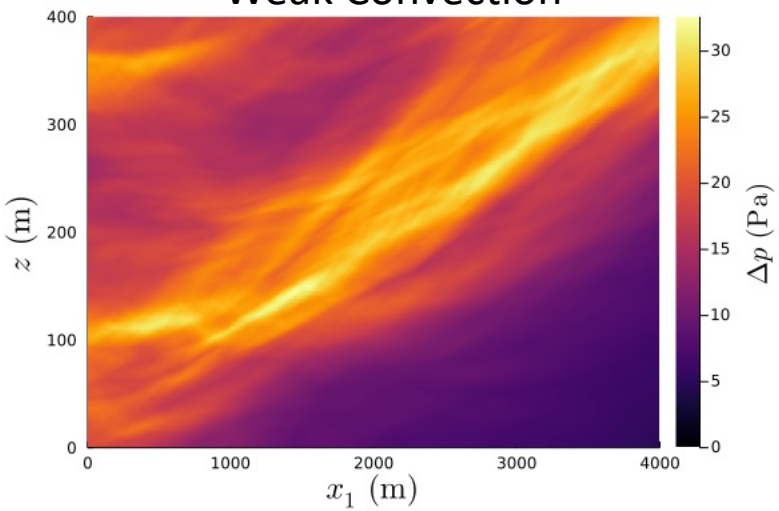

N-wave overpressure beyond the lateral cutoff.

Strong Convection

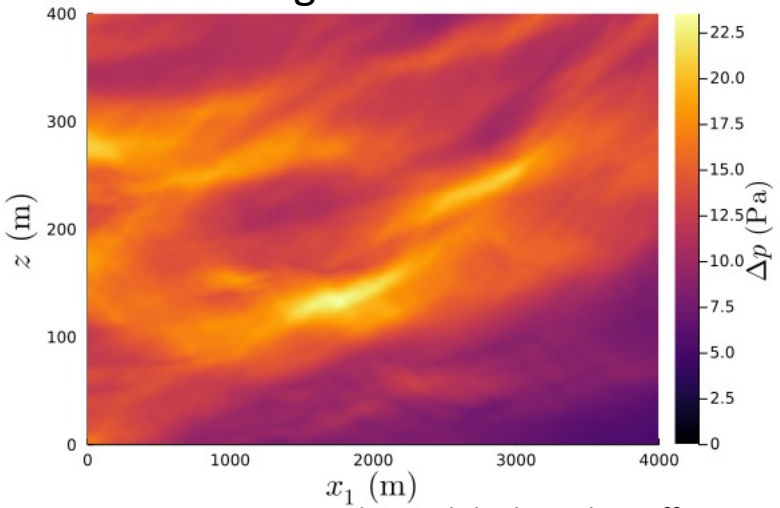

N-wave overpressure beyond the lateral cutoff.

Average N-wave PL beyond cutoff

Convection Level	$\overline{\Delta \mathrm{PL}}$ (1 km)	$\overline{\Delta \mathrm{PL}}$ (2 km)
Weak (KSC20)	-8 dB	-10 dB
Moderate (KSC6)	-5 dB	-6.5 dB
Strong (AFRC3)	-2.5 dB	-5 dB

Average shaped boom PL beyond cutoff

Convection Level	$\overline{\Delta \mathrm{PL}}$ (1 km)	$\overline{\Delta \mathrm{PL}}$ (2 km)
Weak (KSC20)	-12 dB	-14 dB
Moderate (KSC6)	-7.5 dB	-9 dB
Strong (AFRC3)	-2.5 dB	-4.5 dB

Waveforms

- Attenuation, rounding, and phase shift
- Post-boom fluctuations not significant for weak convection
- Considerable turbulence effects for strong convection

N-waves

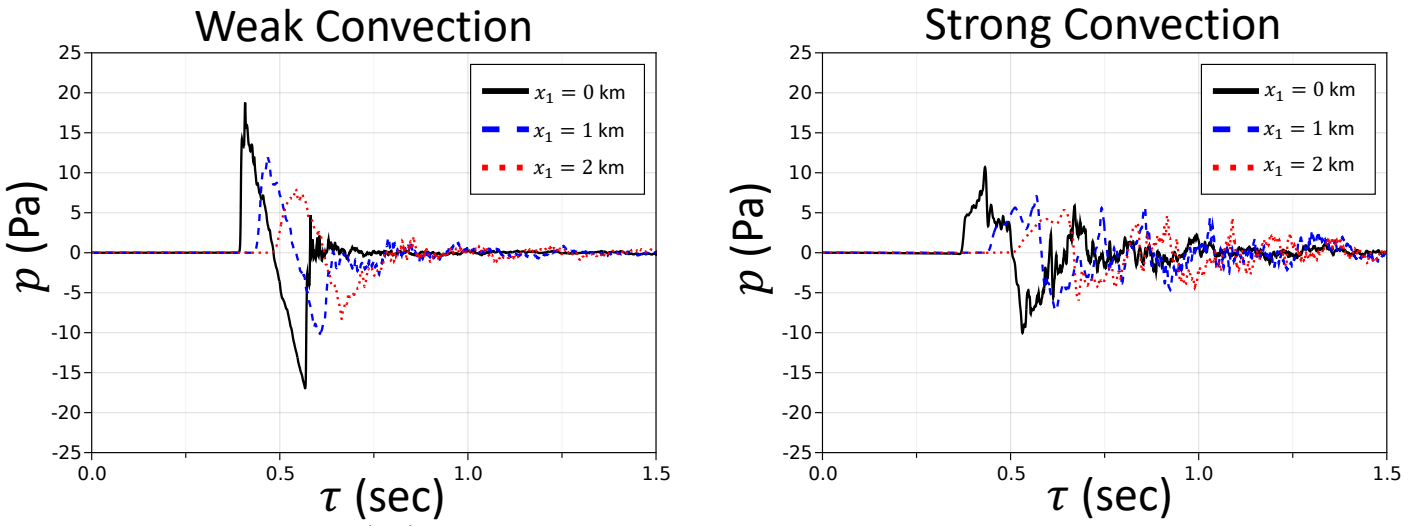

N-waves at 3 different locations in the shadow zone for weak and strong convection.

Shaped booms

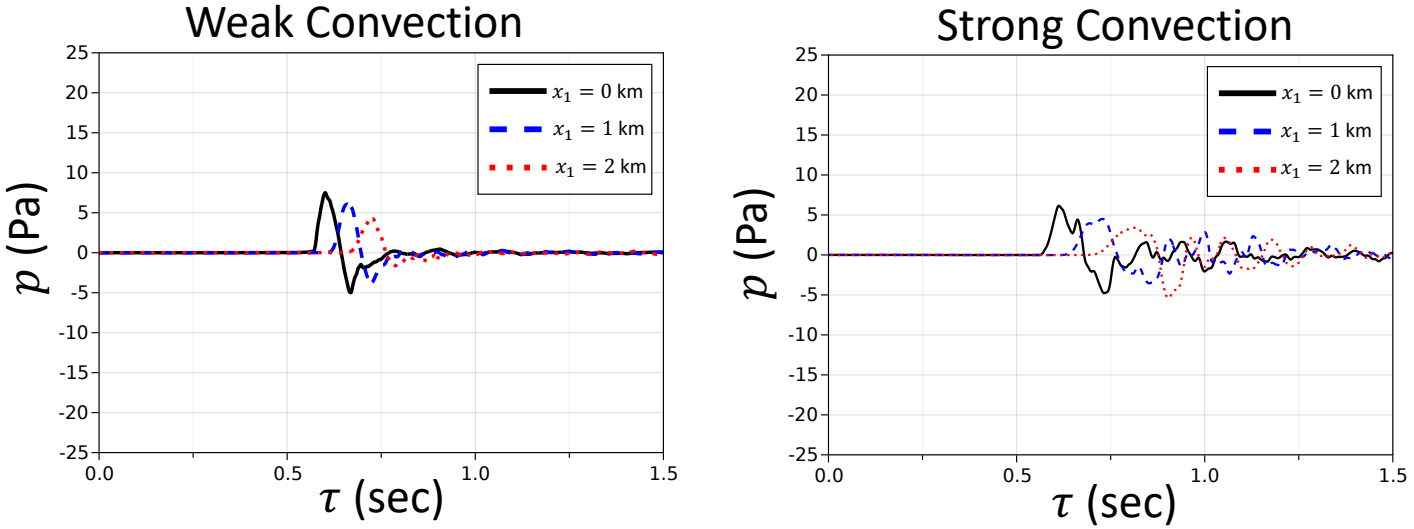

Shaped booms at 3 different locations in the shadow zone for weak and strong convection.

Loudness Variability

- $\sigma_{\Delta \mathrm{PL}}$ is generally between 1 – 3 dB
- $\sigma_{\Delta \mathrm{PL}}$ is larger on average for shaped boom
- Loudness variability for weak convection is larger near cutoff
- Moderate and strong convection cases undergo significant turbulent distortion during propagation to lateral cutoff

N-wave

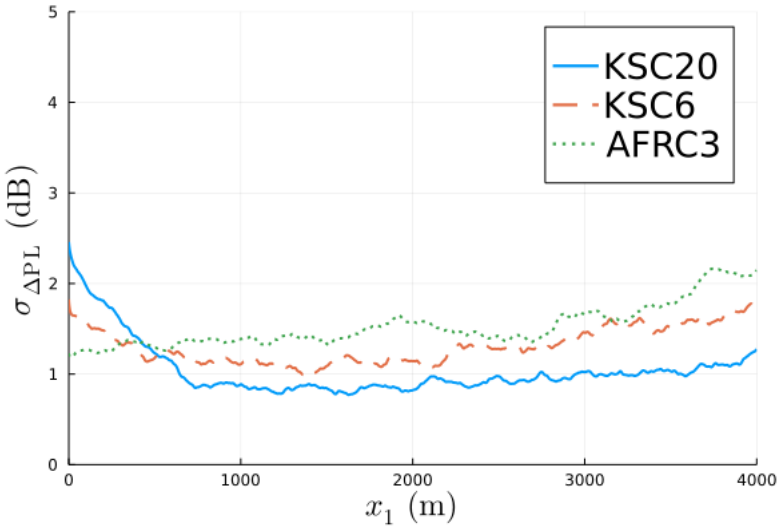

Standard deviation of PL for the N-wave at each ABL condition.

Shaped boom

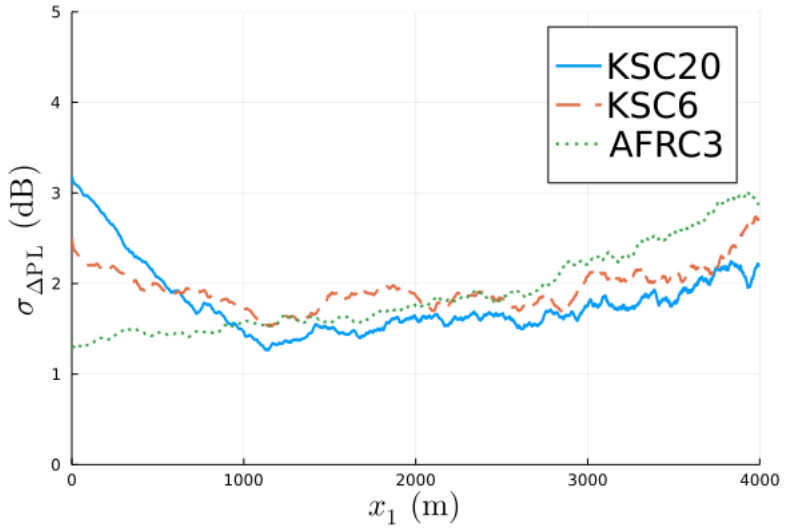

Standard deviation of PL for the shaped boom at each ABL condition.

Summary

- Prediction method developed with new propagation tool (sbABL) to account for turbulence effects
  - Interfaces with existing propagation code (PCBoom)
  - Capable of simulating N-waves and shaped booms beyond lateral cutoff
  - Inhomogeneous ABL turbulence in unstable conditions (sunny day)
- Simulations through weak, moderate, and strong convection indicate
  - As convection level increases, $\overline{\Delta \mathrm{PL}}$ beyond cutoff increases (true for other metrics)
  - $\sigma_{\Delta \mathrm{PL}}$ is generally between 1 – 3 dB for both waveforms

Questions?

Thank you

References

1. K. J. Plotkin, M. Downing, J. Page, “USAF single event sonic boom prediction model: PCBOOM,” The Journal of the Acoustical Society of America, vol. 95, no. 5, pp. 2839–2839, May 1994. doi:10.1121/1.409605.
2. S. K. Rallabhandi, “Advanced sonic boom prediction using the augmented burgers equation,” Journal of Aircraft, vol. 48, no. 4. American Institute of Aeronautics and Astronautics (AIAA), pp. 1245–1253, Jul 2011. doi: 10.2514/1.c031248.
3. T. Stout, Simulation of N-wave and shaped supersonic signature turbulent variations, Ph.D. dissertation, Pennsylvania State University, 2018.
4. F. Dagrau, M. Rénier, R. Marchiano, F. Coulouvrat, “Acoustic shock wave propagation in a heterogeneous medium: A numerical simulation beyond the parabolic approximation,” The Journal of the Acoustical Society of America, vol. 130, no. 20, pp. 20–32. Jul 2011. doi:10.1121/1.3583549.
5. D. Luquet, R. Marchiano, F. Coulouvrat, “Long range numerical simulation of acoustical shock waves in a 3d moving heterogeneous and absorbing medium,” Journal of Computational Physics, vol. 379, pp. 237–261, Feb 2019. doi:10.1016/j.jcp.2018.11.041.
6. A. N. Carr, J. B. Lonzaga, S. A. E. Miller, “Numerical prediction of loudness metrics for N-waves and shaped sonic booms in kinematic turbulence,” The Journal of the Acoustical Society of America, vol. 151, no. 6, pp. 3580–3593, Jun 2022. doi:10.1121/10.0011514.
7. A. Loubeau, S. R. Wilson, and J. Rathsam, “Updated evaluation of sonic boom noise metrics,” The Journal of the Acoustical Society of America, vol. 144, no. 3, pp. 1706–1706, Sep. 2018. [Online]. Available: https://doi.org/10.1121/1.5067578

References

8. J. A. Page, K. K. Hodgdon, P. Krecker, R. Cowart, C. Hobbs, C. Wilmer, C. Koening, T. Holmes, T. Gaugler, D. L. Shumway, J. L. Rosenberger, and D. Philips, “Waveforms and sonic boom perception and response (WSPR): low-boom community response program pilot test design, execution, and analysis,” National Aeronautics and Space Administration, Langley Research Center, Tech. Rep. NASA/CR-2014-218180, 2014.
9. J. A. Page, K. H. Hogdon, R. P. Hunte, D. E. Davis, T. A. Gaugler, R. Downs, R. A. Cowart, D. J. Maglieri, C. Hobbs, G. Baker, M. Collmar, K. A. Bradley, B. Sonak, D. Crom, and C. Cutler, “Quiet supersonic flights 2018 (QSF18) test: Galveston, Texas risk reduction for future community testing with a low-boom flight demonstration vehicle,” National Aeronautics and Space Administration, Langley Research Center, Tech. Rep. NASA/CR–2020-220589, 2020.
10. K. A. Bradley, C. M. Hobbs, C. B. Wilmer, V. W. Sparrow, T. A. Stout, J. M. Morgenstern, K. H. Underwood, D. J. Maglieri, R. A. Cowart, M. T. Collmar, H. Shen, P. Blanc-Benon, “Sonic booms in atmospheric turbulence (SonicBAT): The influence of turbulence on shaped sonic booms,” NASA Tech. Rep. NASA/CR-2020-220509, 2020.
11. L. J. Cliatt, M. A. Hill, and E. Haering, “Mach cutoff analysis and results from NASA’s farfield investigation of no-boom thresholds,” in 22nd AIAA/CEAS Aeroacoustics Conference, American Institute of Aeronautics and Astronautics, AIAA 2016-3011, May 2016, [Online]. Available: https://doi.org/10.2514/6.2016-3011
12. L. J. Cliatt, E. Haering, S. R. Arnac, and M. A. Hill, “Lateral cutoff analysis and results from NASA’s farfield investigation of no-boom thresholds,” Armstrong Flight Research Center, Edwards, California, Tech. Rep. NASA/TM—2016–218850, Feb 2016.
13. F. Coulouvrat, “New equations for nonlinear acoustics in a low Mach number and weakly heterogeneous atmosphere,” Wave Motion, vol. 49, no. 1, pp. 50–63, Jan 2012. doi:10.1016/j.wavemoti.2011.07.002

References

14. V.E. Ostashev, Acoustics in Moving Inhomogeneous Media, E & FN Spon, London, 1997.
15. J. Goodman, Introduction to Fourier optics. Englewood, Colo: Roberts & Co, 2005.
16. F. Coulouvrat, “A quasi-analytical shock solution for general nonlinear progressive waves,” Wave Motion, vol. 46, no. 2, pp. 97–107, Mar 2009. [Online]. Available: https://doi.org/10.1016/j.wavemoti.2008.09.002
17. A. S. Monin and A. M. Obukhov, “Osnovnye zakonomernosti turbulentnogo peremeshivanija v prizemnom sloe atmosfery (basic laws of turbulent mixing in the atmosphere near the ground),” Trudy geofiz. inst. AN SSSR 24(151), vol. 24, no. 151, p. 163–187, 1954.
18. V.E. Ostashev, D. K. Wilson, Acoustics in moving inhomogeneous media, CRC Press, Taylor & Francis Group, Boca Raton, FL, 2016.
19. J. L. Lumley, “The structure of inhomogeneous turbulent flows,” Atmospheric Turbulence and Radio Wave Propagation, Nauka, Moscow, 1967, pp. 166-178.
20. D. K. Wilson, “Turbulence models and the synthesis of random fields for acoustic wave propagation calculations.,” Technical Report ARL-TR-1677, Army Research Laboratory, Adelphi, MD, 1998.
21. D. K. Wilson, “A turbulence spectral model for sound propagation in the atmosphere that incorporates shear and buoyancy forcings,” The Journal of the Acoustical Society of America, vol. 108, no. 5, pp. 2021–2038, 2000. doi:10.1121/1.1311779.

Abstract

➢ Recent flight tests during the Quiet Supersonic Flights 2018 (QSF18) study reported sonic booms heard outside of the primary carpet region. In the absence of turbulence, the lateral cutoff region separates the primary sonic boom carpet from the shadow zone, where the sonic boom signal experiences significant attenuation. However, when turbulence is present in the atmospheric boundary layer (ABL), additional scattering of the sonic boom to the shadow zone region occurs. A method is presented for simulating sonic boom propagation in a turbulent atmospheric boundary layer beyond the lateral cutoff region into the shadow zone. A split-step method is used to integrate a partially one-way equation for the acoustic pressure. Inhomogeneous turbulence, representative of the ABL, is generated in the computational domain with a Fourier synthesis approach. Distributions of several loudness metrics in the shadow zone region for a sonic boom N-wave and a shaped boom are examined. Increasing both turbulence root-mean-square velocity and integral length scale are found to increase the average loudness of booms in the shadow zone. (This research is supported by the Commercial Supersonic Technology Project of the National Aeronautics and Space Administration under Grant No. 80NSSC19K1685.)

Extra Slides

Angular Spectrum Method

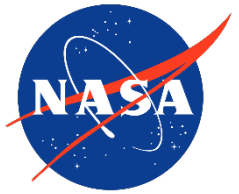

- Helmholtz Eqn. in delayed time

$$\frac{2i\omega}{c_0}\frac{\partial \hat{p}}{\partial x_1} = \frac{\partial^2 \hat{p}}{\partial x_1^2} + \frac{\partial^2 \hat{p}}{\partial x_2^2}$$

- Take cosine transform in x_2 (sound hard boundary)
- Finite impedance boundaries
  - Combination of cosine and sine transform [15,16]
  - Not considered here
- Angular spectrum, $A(x_1, k_2, \omega) = \int_0^\infty \hat{p}(x_1, x_2, \omega)\cos(k_2 x_2)dx_2$
- Evolution governed by

$$\frac{d^2A}{dx_1^2} - \frac{2i\omega}{c_0}\frac{dA}{dx_1} - k_2^2 A = 0$$

Turbulence Statistics of Generated Fields

- Synthetically generated turbulence statistics for weak and strong convection
- 750 fields generated for each case

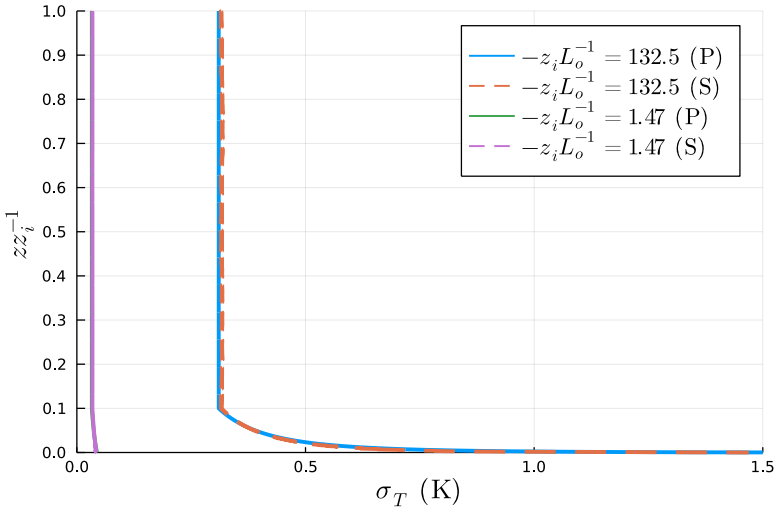

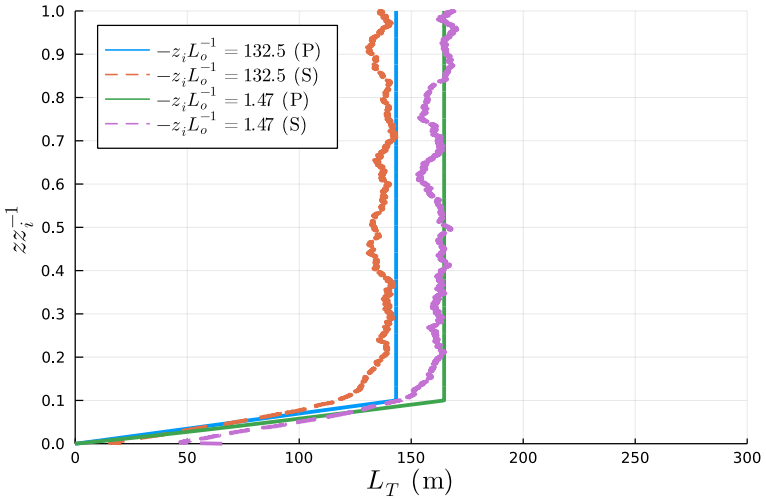

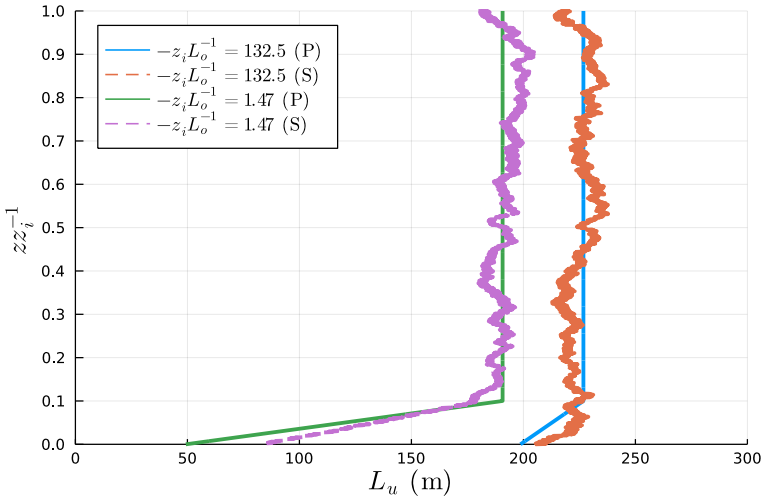

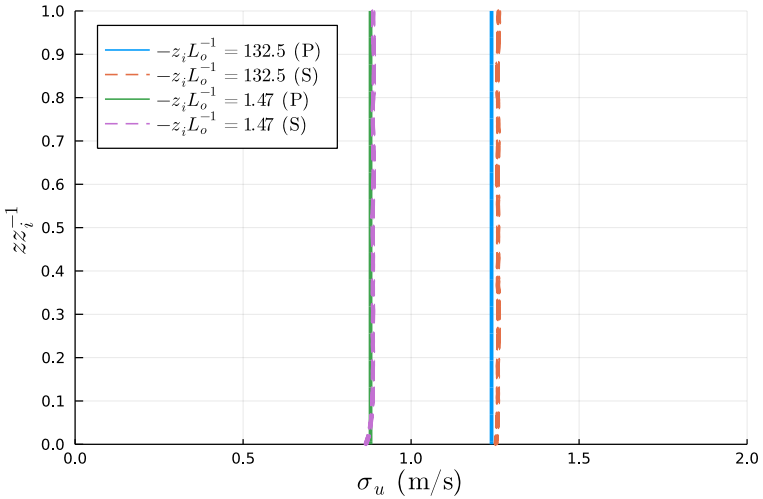

Probability Distributions Strong Convection

- PL distributions for both waveforms
- Skewness present for strong convection conditions
- No skewness in KSC setpoints up to 2 km beyond cutoff

N-wave, Strong Convection

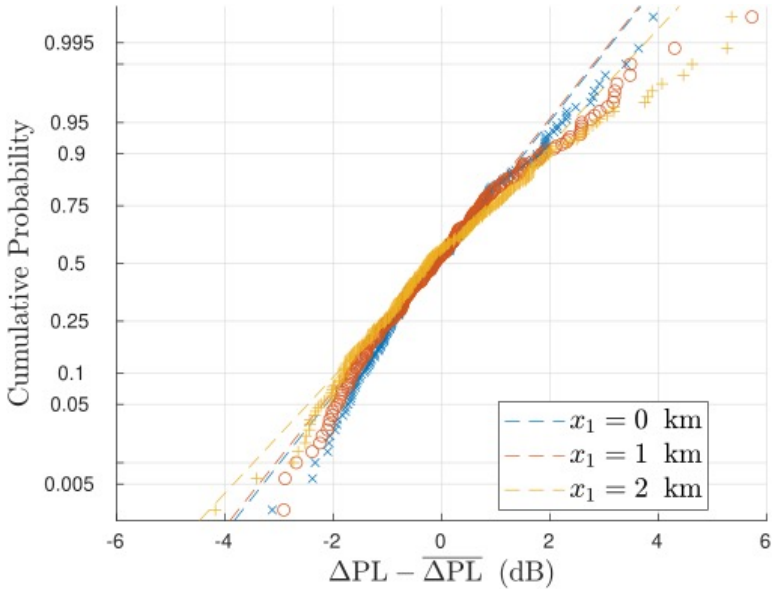

PL distribution for N-wave at 3 locations beyond the cutoff in strong convection conditions.

Shaped Boom, Strong Convection

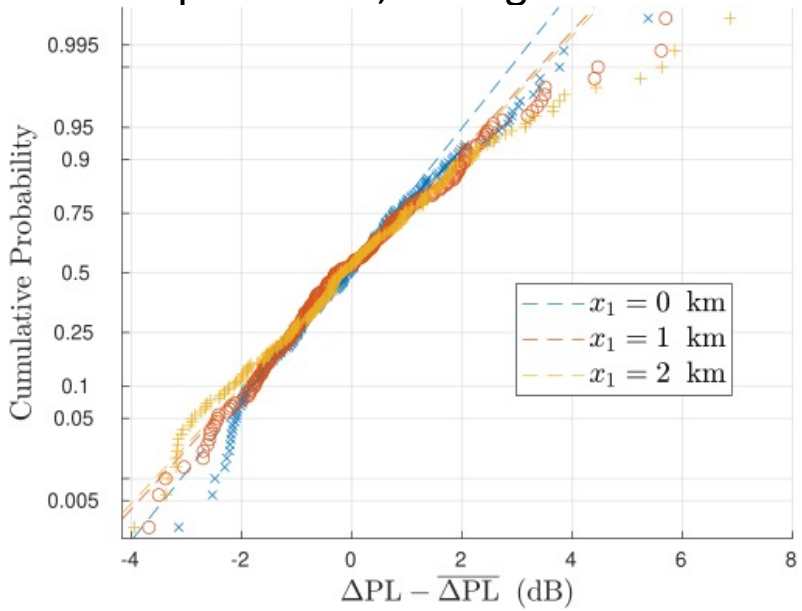

PL distribution for shaped boom at 3 locations beyond the cutoff in strong convection conditions.

PL Distributions Weak Convection

- PL distributions at weak convection levels (KSC20) beyond cutoff
- Distributions are well approximated by a normal distribution

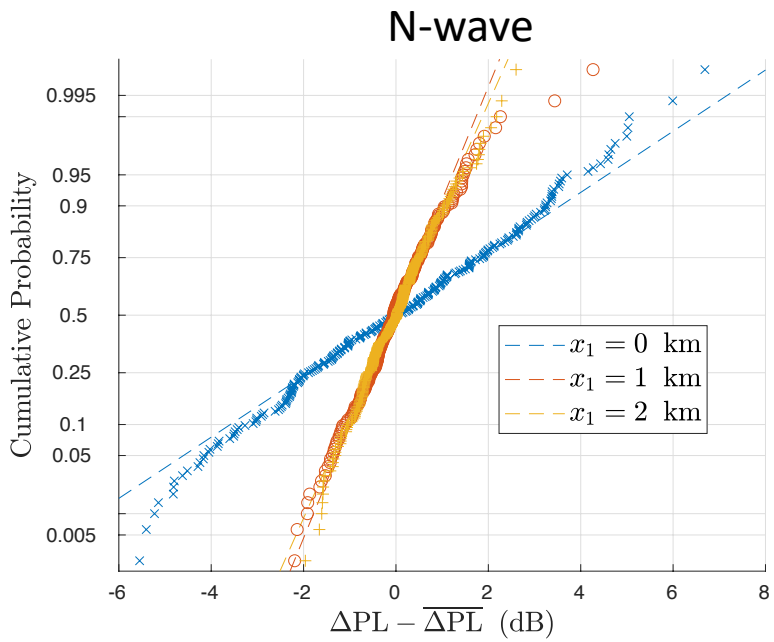

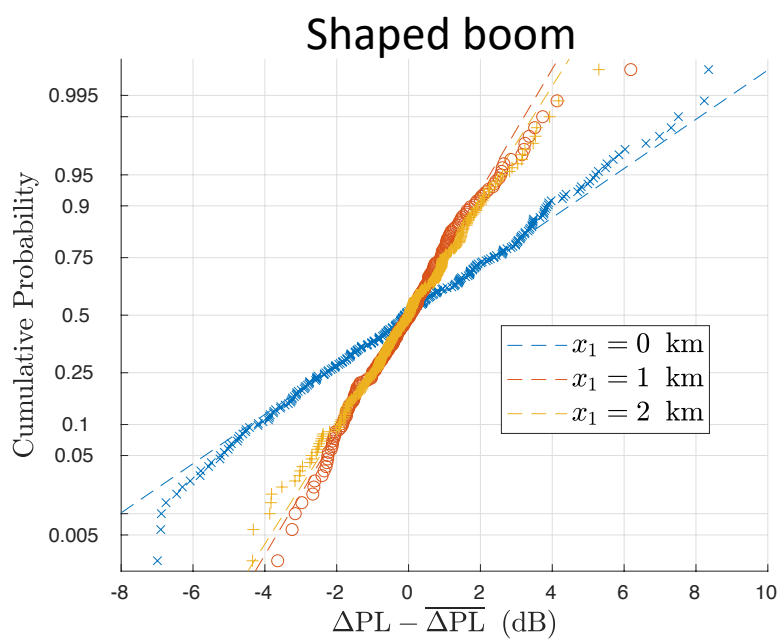

PL Distributions Moderate Convection

- PL distributions at moderate convection levels (KSC6) beyond cutoff
- N-wave distribution is slightly skewed beyond 1 km